MDPI

Article

Computational Imaging for Simultaneous Image Restoration and Super-Resolution Image Reconstruction of Single-Lens Diffractive Optical System Supplementary File

Kai Liu [1,2], Xiao Yu [1], Yongsen Xu [1], Yulei Xu [1,*], Yuan Yao [1], Nan Di [3], Yefei Wang [1], Hao Wang [1], Honghai Shen [1]

[1] Key laboratory of Airborne Optical Imaging and Measurement, Changchun Institute of Optics, Fine Mechanics and Physics, Chinese Academy of Sciences, Changchun, 130033, China; liukai174@mails.ucas.edu.cn(K.L.); pm13l@sina.com(Y.X.); m13324473070@163.com(X.Y.); wanghao7600@163.com(H.W.);c8george@sina.com(Y.Y.);shenhh@ciomp.ac.cn(H.S.)

[2] University of Chinese Academy of Sciences, Beijing, 100049,China;

[3] Academy for Advanced Interdisciplinary Studies,Northeast Normal University,Changchun 130024,Jilin province,China

* Correspondence: yuleixu@ciomp.ac.cn; Tel.: +86-1384-406-5873

1. Point spread function of the HDOE

We set the design center wavelength ($\lambda_0 = 555nm$), and set the diffraction order of the center wavelength to the 10th order($m = 10$). The phase function of the HDOE is optimized as a continuous and increasing higher-order term function in commercial optical design software, which can be expressed as:

$$\varphi(r)\mathrm{m}\sum_{\mathrm{i}=1}^{\mathrm{N}} A_i r^{2i}, \tag{1}$$

where, m is a constant that represents the diffraction design order of the center wavelength; N is the order of the phase function; A_i is the corresponding coefficient of the order i; r is the radial coordinate of HDOE. A more detailed description is in the Supplementary file.

The process of calculating the surface height function from the HDOE phase function is shown in **Figs**1. The phase function of HDOE will be compressed within [0, $2m\pi$], thence, the compressed phase function is expressed as:

$$\varphi_0(r) = mod_{2m\pi}\left(\varphi_p(r)\right), \tag{2}$$

where,$mod(\cdot)$is the remainder function.

At the center wavelength λ_0, the refractive index of the corresponding optical material is n_{λ_0}, then the height function of the relief microstructure of the harmonic diffractive optical element is:

$$h_0(r) = \frac{m\lambda_0}{n_{\lambda_0} - 1} \cdot \frac{1}{2\pi} \cdot \varphi_0(r), \tag{3}$$

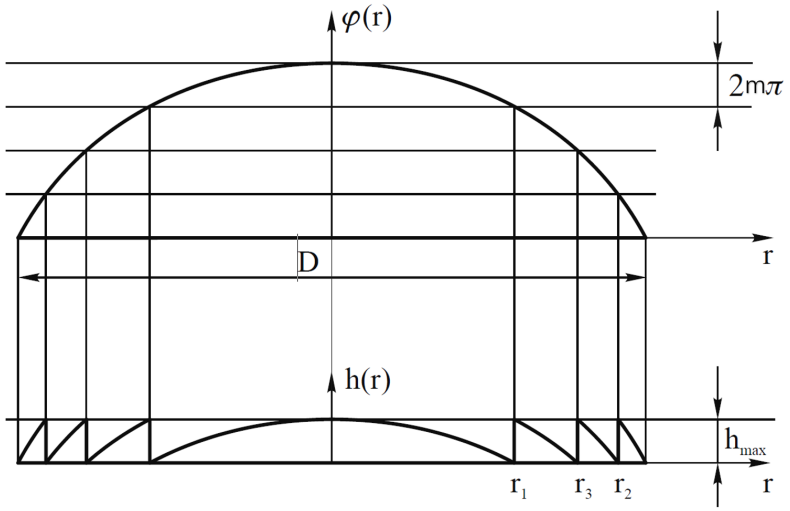

Figure S1. Schematic diagram of HDOE phase function and height function.

Transform the height function of HDOE$h_0(r)$ into an equation in the Cartesian coordinate system$h(x', y')$, where the coordinate system (x′,y′) plane is the HDOE plane, the origin of the coordinates is its center,as shown in **Fig**S2. thence,$r^2 = x'^2 + y'^2$, the height function can be expressed as:

$$h(x', y') = h_0(\sqrt{x'^2 + y'^2}) \tag{4}$$

Substitute **eq**(1), (2), (3) into **eq** (4):

$$\begin{aligned} h(x, y) &= h_0(\sqrt{x'^2 + y'^2}) \\ &= \frac{\mathrm{m}\lambda_0}{n_{\lambda_0} - 1} \cdot \frac{1}{2\pi} \cdot mod_{2m\pi}(\varphi(\sqrt{x'^2 + y'^2})) \end{aligned} \tag{5}$$

The phase delay function of the complex amplitude wavefield of HDOE is proportional to its thickness $h(x, y)$, thence, the phase delay function of the harmonic diffractive optical element can be deduced:

$$\phi_{HDOE,\lambda}(x', y') = \frac{2\pi(n_\lambda - 1)}{\lambda} h(x', y') \tag{6}$$

Thence, λ is the wavelength of the incident light wave, n_λ is the refractive index of the corresponding optical material when the wavelength of the light wave is λ, as shown in **Fig**S2. It is worth noting that λ is not the design center wavelength of the harmonic diffractive optical elementλ_0.

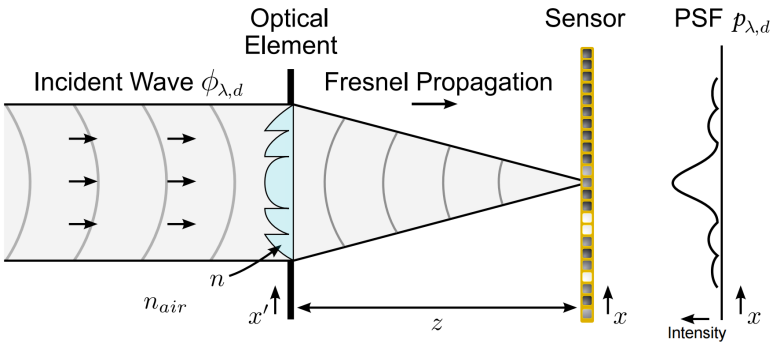

Figure S2. PSF model of multi-order diffractive lens based on differentiable Fresnel diffraction theory [4].

The point spread function of HDOE can be derived according to the Fresnel diffraction propagation theory[1].As shown in **FigS**2, a point light source with a wavelength of λ and a phase of $\phi_{\lambda,d}$ at a distance of d from the optical element is incident on the aperture plane of the HDOE (refractive index is n_λ) superior.HDOE changes the phase of the incident wavefront, and the generated wavefront is focused on the sensor image surface from the aperture according to the Fresnel diffraction propagation theory, and the distance between HDOE and the detector is z. The wavefield complex amplitude function of the incident wavefront of the sensor is u_λ. The plane where the harmonic diffractive optical element is located is (x′, y′), and the plane where the detector is located is (x, y).

A light wave with amplitude A and phase $\phi_{d,\lambda}$ is incident on the HDOE, and the wave field will be affected as[1]:

$$U_\lambda(x', y', z = 0) = A(x', y')e^{i[\phi_{d,\lambda}(x',y') + \phi_{HDOE,\lambda}(x',y')]} \tag{7}$$

where,$U_\lambda(x', y', z = 0)$is the complex amplitude function of the wave field after the light wave passes through the HDOE, also known as the complex transmission function,$i$is the light wave propagation constant, referred to as the wave number for short,$i = 2\pi/\lambda$.

According to the Fresnel diffraction propagation theory, after the light field propagates to a distance z in free space, its field distribution is:

$$U_\lambda(x, y, z) = \frac{e^{ikz}}{i\lambda z} \iint U_\lambda(x', y', 0)e^{\frac{ik}{2z}[(x-x')^2+(y-y')^2]}dx'dy' \tag{8}$$

SHDCI is similar to a telescope imaging system, so the plane wave hypothesis is proposed, that is, light waves emitted by a point light source at infinity enter the optical system. In this case, incident light from a light source along the optical axis can be described as a plane wave with constant amplitude A and constant phase ϕ_0. Therefore, the complex amplitude function of the wave field arriving on the image plane can be simplified as:

$$U_\lambda(x, y, z) = \frac{e^{ikz}}{i\lambda z} \iint Ae^{i[\phi_0 + \phi_{HDOE,\lambda}(x',y')]}e^{\frac{ik}{2z}[(x-x')^2+(y-y')^2]}dx'dy' \tag{9}$$

$$U_\lambda(x, y, z) = \frac{e^{ikz}}{i\lambda z} \cdot Ae^{i\phi_0} \iint e^{i[\phi_{HDOE,\lambda}(x',y')]}e^{\frac{ik}{2z}[(x-x')^2+(y-y')^2]}dx'dy' \tag{10}$$

The point spread function h(x,y) of HDOE is the unit-normalized representation of the squared intensity of the wavefieldU_λ[1]:

$$\begin{aligned} h_1(x, y) &= |U_\lambda|^2 \\ &= \left| \cdot \mathbf{F}\{U_\lambda(x', y', 0)e^{\frac{ik}{2z}[(x-x')^2+(y-y')^2]}\} \right|^2 \end{aligned} \tag{11}$$

Thence, it can be assumed that the amplitude A=1, and the field distribution function on the image surface is:

$$U_\lambda(x, y, z) = \frac{e^{ikz}}{i\lambda z} \cdot \iint t_{HDOE,\lambda}(x', y')e^{\frac{ik}{2z}[(x-x')^2+(y-y')^2]}dx'dy', \tag{12}$$

where, $t_{HDOE,\lambda}$ is the complex transmittance function of HDOE, $t_{HDOE,\lambda} = e^{i[\phi_{HDOE,\lambda}(x',y')]}$.

When the diffraction efficiency of the light wave decreases, a part of the energy will be scattered and distributed on the image plane, forming stray light background radiation.Therefore, the generalized pupil function of HDOE can be divided into two parts; the main part is the pupil function of the designed diffraction order for focusing$P_{HDOE,\lambda}(x', y')$; the other part is the stray light background radiation pupil function$P_{BG}(x', y')$ caused by

the light wave in the non-design order diffraction.The generalized pupil function can be expressed as:

$$\begin{aligned} P(x',y') &= P_{HDOE,\lambda}(x',y') + P_{BG}(x',y') \\ &= t_{HDOE,\lambda}(x',y') \exp\left[i\frac{k}{n'}\phi_0(x',y')\right] \\ &+ t_{\mathrm{BG}}(x',y') \exp\left[i\frac{k}{n'}\phi_0(x',y')\right] \end{aligned} \tag{13}$$

The light field intensity function of the HDOE imaging system can be written as the superposition of the focusing impulse response $h_1(x,y)$ and the background impulse response h_{BG}:

$$\begin{aligned} I(x,y) = |h_1(x,y)|^2 + |h_{\mathrm{BG}}(x,y)|^2 + h_1^*(x,y)h_{\mathrm{BG}}(x,y) \\ + h_1(x,y)h_{\mathrm{BG}}^*(x,y), \end{aligned} \tag{14}$$

where, * represents the complex conjugate term. Note the cross term in the intensity expression given by the **eq**(14). The expansion direction of the main impulse response function and the background impulse response function in the time domain is very different. Therefore the value of the cross term is small and the effect on the intensity at the image point (x, y) is negligible. So we can simplify the light field intensity function to:

$$I(x,y) = |h_1(x,y)|^2 + |h_{\mathrm{BG}}(x,y)|^2 \tag{15}$$

The point spread function of HDOE is a normalized representation of the light field intensity function,and the normalization process can be expressed as[2,3]:

$$h(x,y) = |I(x,y)|_1 = \left||h_1(x,y)|^2 + |h_{\mathrm{BG}}(x,y)|^2\right|_1 \tag{16}$$

$$\int_{-\infty}^{\infty}\int_{-\infty}^{\infty}\left|h_1^1(x,y)\right|^2 \mathrm{d}x\,\mathrm{d}y + \int_{-\infty}^{\infty}\int_{-\infty}^{\infty}\left|h_{\mathrm{BG}}^1(x,y)\right|^2 \mathrm{d}x\,\mathrm{d}y = 1 \tag{17}$$

Where, part of the equation can be further simplified:

$$\int_{-\infty}^{\infty}\int_{-\infty}^{\infty}\left|h_1^1(x,y)\right|^2 \mathrm{d}x\,\mathrm{d}y = \frac{1}{A_{\mathrm{pupil}}}\int_{-\infty}^{\infty}\int_{-\infty}^{\infty}|h_1(x,y)|^2 \mathrm{d}x\,\mathrm{d}y, \tag{18}$$

where A_{pupil} is the pupil area. The integral of the principal impulse response function of HDOE over the pupil area is its diffraction efficiency, which is expressed as:

$$\eta_{\mathrm{HDOE}} = \frac{1}{A_{\mathrm{pupil}}}\int_{-\infty}^{\infty}\int_{-\infty}^{\infty}\left|t_1(x',y')\right|^2 \mathrm{d}x'\,\mathrm{d}y' \tag{19}$$

Thence, the point spread function of the HDOE in the wide bandwidth spectrum can be further simplified as:

$$h(x,y) = \eta_{\mathrm{HDOE}}h_1(x,y) + (1-\eta_{\mathrm{HDOE}})h_{\mathrm{BG}}(x,y) \tag{20}$$

The diffraction of light waves at the design order is used for imaging, and the point spread function will be concentrated at a point in the spatial domain. However, its non-design sub-diffraction forms extremely out-of-focus background stray light, and the point spread function spreads out in the spatial domain. Consequently, it can be inferred that the spread of the background radiation point spread function is very low at the spatial frequency close to zero. In order to easily calculate the point spread function of the

diffractive optical system, we can approximate it as the unit pulse function. The impulse response function of the background radiation is approximated as:

$$h_{BG}(x',y') = \int_{-\infty}^{\infty}\int_{-\infty}^{\infty}(1-\eta_1)\delta(x-x',y-y')dx'dy' \tag{21}$$

In summary, the imaging degradation model of HDOE can be expressed as:

$$g = h(x,y) * f + n \tag{22}$$

where, f is the ground truth, g is the degraded image, and n is the system noise.It can also be expressed as:

$$g = [\eta_{\mathrm{HDOE}} h_1(x,y) + (1-\eta_{\mathrm{HDOE}})h_{\mathrm{BG}}(x,y)] * f + n \tag{23}$$

2. DDZMR network for image denoising task

To verify the contribution of image denoising in the DDMZR network, the performance of DDMZR denoising is tested on a public test dataset SIDD[5]. As shown in **Fig.** S3, most of the noise on the image has been effectively removed, and the detailed texture of the image has been preserved and restored. The average value of peak signal-to-noise ratio (PSNR) and image structure similarity (SSIM) measurements before and after the image is processed by the MZDDR network is shown in **TabS**1.

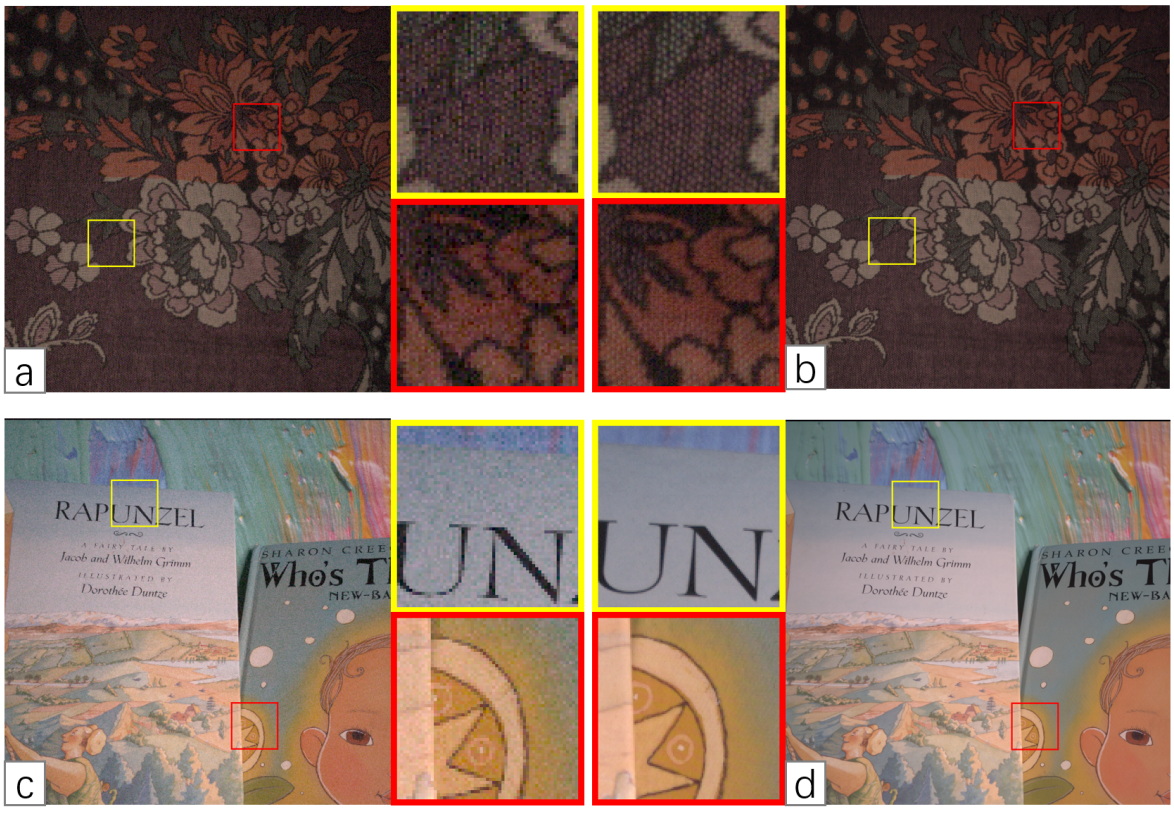

Figure S3. Image denoising test for testing the DDZMR network on the SIDD dataset; (a)(c), the original image with a lot of noise; (b)(d), the image processed by the DDZMR network.

Table S1. Comparison of PSNR and SSIM before and after image denoising with MZDDR network.

	PSNR	SSIM
High noise image	23.63	0.8133
Image reconstructed by MZDDR network	31.01	0.9004

3. Comparison of the performance of DDZMR and CARN processing images captured by SHDCIS

To verify the performance advantage of the DDMZR network over the CARN network, the CARN network is tested using the raw images captured by SHDCIS. And compared with images processed by DDZMR network. It is evident from **Fig.** S4 that the super-resolution processing of strongly degraded images by CARN is poor compared to DDZMR. DDZMR can restore degraded images and perform image super-resolution at the same time, which is the ability that CARN does not have. Images in HDOE imaging are severely degraded. Since CARN cannot effectively recover degraded images, it is not satisfactory in super-resolution processing of images captured by SHDCIS.

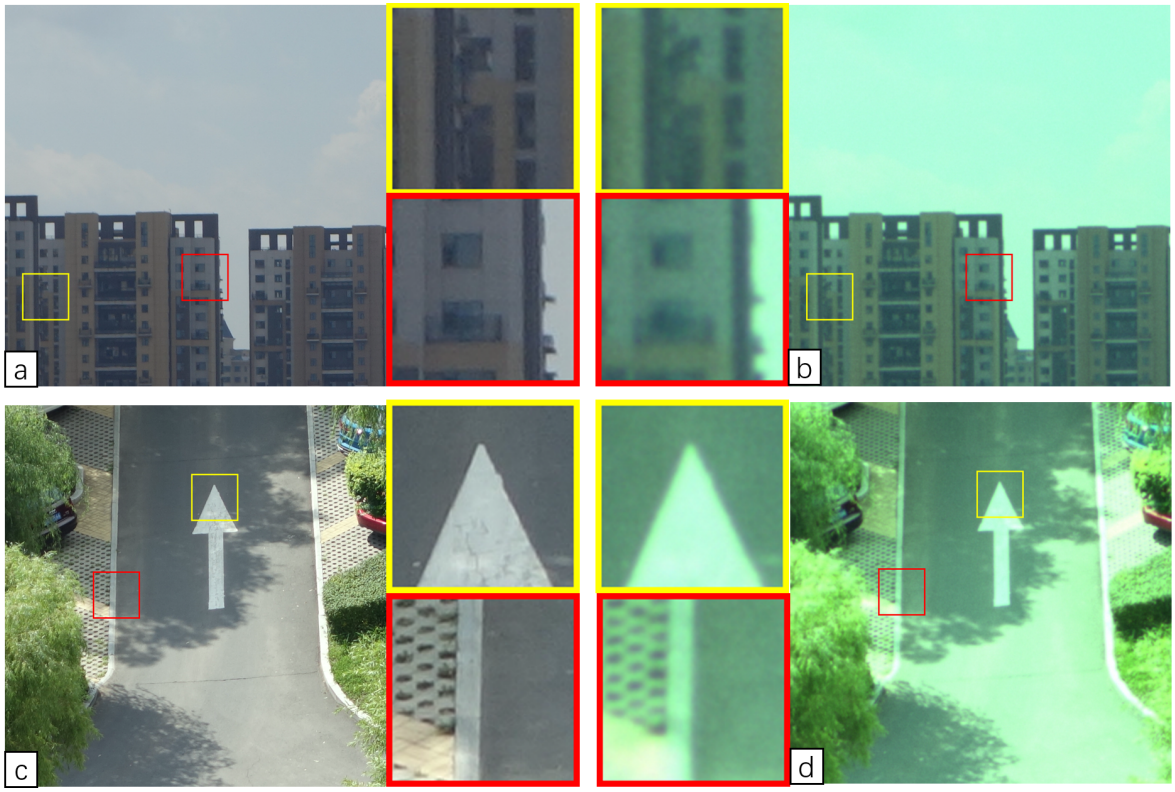

Figure S4. Comparison of the performance of DDZMR and CARN processing images captured by SHD-CIS; (a) (c), the DDZMR computationally reconstructed images; (b) (d), the CARN computationally reconstructed images.

References

1. Joseph, W. Introduction To Fourier Optics 3rd Edition 2007 Joseph W. 2021.
2. Wang, D.; Zhi, X.; Zhang, W.; Yin, Z.; Jiang, S.; Niu, R. Influence of ambient temperature on the modulation transfer function of an infrared membrane diffraction optical system. *Applied optics* **2018**, *57 30*, 9096–9105.
3. Buralli, D.A.; Morris, G.M. Effects of diffraction efficiency on the modulation transfer function of diffractive lenses. *Applied optics* **1992**, *31 22*, 4389–96.
4. Sitzmann, V.; Diamond, S.; Peng, Y.; Dun, X.; Boyd, S.P.; Heidrich, W.; Heide, F.; Wetzstein, G. End-to-end optimization of optics and image processing for achromatic extended depth of field and super-resolution imaging. *ACM Transactions on Graphics (TOG)* **2018**, *37*, 1 – 13.

5. Abdelhamed, A.; Lin, S.; Brown, M.S. A High-Quality Denoising Dataset for Smartphone Cameras. *2018 IEEE/CVF Conference on Computer Vision and Pattern Recognition* **2018**, pp. 1692–1700.